JOURNAL OF OPTOELECTRONICS AND ADVANCED MATERIALS Vol. 9, No. 3, March 2007, p. 764 - 767

Nanostructurated materials for hyperthermia treatment of bone tumors

C. MIRESTEAN*, H. MOCUTA, R. V. F. TURCU, G. BORODI[a], S. SIMON
Faculty of Physics, Babes-Bolyai University, Cluj-Napoca 400084, Romania
[a]*National Institute for R&D of Isotopic and Molecular Technologies R-400293, Cluj-Napoca, Romania*

Sol-gel method has been used for obtaining polycrystalline iron containing hydroxyapatite materials usable for hyperthermia. In calcium phosphate sol-gel glasses with Ca/P ratio of 1.67, like that in hydroxyapatite, the bone mineral phase was introduced up to 5 mol% Fe_2O_3. X-ray diffraction (XRD) analysis evidenced the growth of hydroxyapatite type crystals in the heat treated samples. As was revealed from the width of the main diffraction peak the developed crystals are of nano size after heat treatment at 300 °C. Their size increases with heat treatment time and temperature. After heat treatment at 300°C only in the samples with iron content the crystals remain of hydroxyapatite type, showing that the iron plays a stabilising role in this phase. The phosphorus environment was investigated by Nuclear Magnetic Resonance (NMR). The ^{31}P NMR spectra show that the phosphorus structural units in nanostructurated samples are completely different from those of the samples resulted after higher temperature heat treatment. These results are correlated with the XRD data.

(Received November 15, 2006; accepted December 21, 2006)

Keywords: Hydroxyapatite, X-ray diffraction, NMR, Nanocrystals

1. Introduction

Sol-gel method for oxide systems preparation has attracted much attention in the synthesis of materials used for hyperthermia [1]. These materials show bioactive and magnetic properties and can be used as thermoseeds for hyperthermia treatment of bone tumors [2].

Hydroxyapatite (HA) with the composition $[Ca_{10}(PO)_4(OH)_2]$ is well known as the mineral component of teeth and bones and it has a considerable interest in dental and medical research. [3,4]. Since their introduction in the 1980's, hydroxyapatite coatings on orthopedic implants have gained a wide acceptance in orthopedic surgery [5].

Skeletal deficiencies, due to trauma, tumors or abnormal growth are common that's why surgical intervention and are usually applied to reconstruct damaged areas and to restore mechanical functions [6].

Hydroxyapatite has been used in orthopedics, dentistry and as a drug deliverer, due to its biocompatibility, nontoxicity, the fact that it has excellent osteoconductive ability, it is resorbable, forms similar structure to bone mineral and it bonds directly with the bone [7, 8].

However the properties of hydroxyapatite, especially the mechanical ones are not comparable to physiological bone so the uses in orthopedic/ dental applications have been limited [9]. As a matter of fact the natural bone is a nanocomposite formed from mineral and organic fractions, which together confer mechanical resistance [10]. In order to replicate the natural bone structure, the synthesis of nanosizes hydroxyapatite, had become a very interesting subject in the recent years [7].

The main purpose in the last decades is not only to control the stoichiometry of the synthetic HA, but also to control the crystal size and shape of the powder.. Therefore a number of novel processing routes have been developed, like, hydrolysis of salts [11], electrochemical deposition, sol-gel methods and more recently microemulsion [12]. The sol gel process and the wet precipitation process for HA usually results in a fine grained microstructure, submicron to nanocrystals, fact that makes their acceptance by the host tissue to be better [13].

The aim of this research is to characterize several calcium phosphate powders with different iron concentrations and obtained after treatment treatments at different temperatures. In this paper, the behaviour of the hydroxyapatite powders preparation is explored and discussed in terms of phase transformation and crystal growth. The method chosen to prepare the nanosized samples is the sol – gel method.

The powders were investigated using X-Ray Diffraction (XRD) and Magic Angle Spinning Nuclear Magnetic Resonance (MAS-NMR).

2. Experimental procedure

Samples of hydroxyapatite composition doped with iron (Fe-HA) was prepared using a $Ca(PO_3)_2$ and $Fe(NO_3)_2$ solution (0.2 M) which was added drop wise to a $(NH_4)_2HPO_4$ aqueous solution (0.2 M) under constant stirring at 90°C for three hours; then the precipitate was separated by filtration , washed with boiling deionized water and dried at 120° C for 24.

There were obtained three sets of samples, at different iron concentrations, varying from 0 to 5 % mol. iron oxide, as prepared, treated for 30 minutes at 300 and 710˚C, respectively.

The crystalline phases of the treated and non-treated samples were investigated by XRD with a DRON diffractometer using CuK_α radiation (λ = 1.5418Å).

The average crystallite size was estimated by using the Scherrer equation:

$$D = \frac{k\lambda}{\beta\cos\theta}$$

where D is the crystallite size of the synthesized HA, λ is the wavelength of CuK_α, k is the shape factor equal to 0.9, θ is the diffraction angle of selected line and $\beta = \sqrt{B^2 - b^2}$, where B is the full width at half maximum intensity and b the resolution parameter of the diffractometer (in our case 1.3).

^{31}P MAS NMR spectra were recorded using a Bruker spectrometer, Avance 400 model, operating at 9.4 Tesla. The used probe it was a double resonance, with 15 kHz maximum spinning frequency. All measurements have been carried out at room temperature. The ^{31}P chemical shift is referenced relative to 85% H_3PO_4 water solution as 0 ppm.

3. Results and discussions

XRD patterns for the as prepared samples are shown in Fig. 1.

An important difference between the XRD patterns for the as prepared undoped sample and the doped samples can be observed. The XRD pattern for the undoped sample has been identified and it corresponds to a monetit phase $CaHPO_4$. By adding iron oxide, it can be seen the XRD patterns suffers a quite obvious transformation, transformation which seem to maintain up to 5% iron oxide content sample. The phase had been identified as corresponding to hydroxyapatite. $Ca_{10}(PO)_4(OH)_2$.

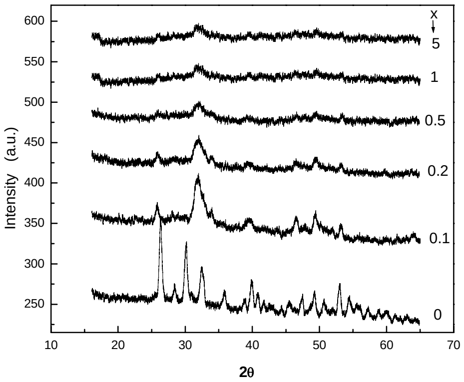

Fig. 1. XRD patterns for the as prepared samples.

The same effect can be observed in the case of hydroxyapatite treated at 300˚C, as the XRD patterns (Fig. 2) are not different from the ones recorded for the untreated samples.

As a conclusion we can say that by adding iron, a change of developed phase occurs so iron plays a HA catalyzing role in this system.

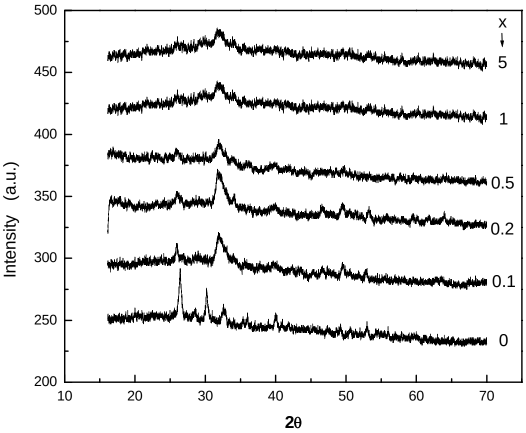

Fig. 2. XRD patterns of the samples after heat treatment at 300 ℃.

After heat treatment at 710˚C completely different diffractograms have been observed for the resulted samples (Fig. 3). The phase identified was of calcium iron phosphate $Ca_9FeH(PO_4)_7$ type [14]. Here unlike in case of the as prepared and 300°C treated samples there isn't any notable difference between the XRD patterns.

In order to estimate the crystallite size of the particles, XRD has been used, due to the fact that the profiles of X-ray powder diffraction peaks reflect the dimension monocrystalline domains.

The crystallite sizes were estimated by using the Scherrer equation and the values are about 20 nm for hydroxyapatite phase, 100 nm for monetit phase and about 10 μm for the calcium iron phosphate.

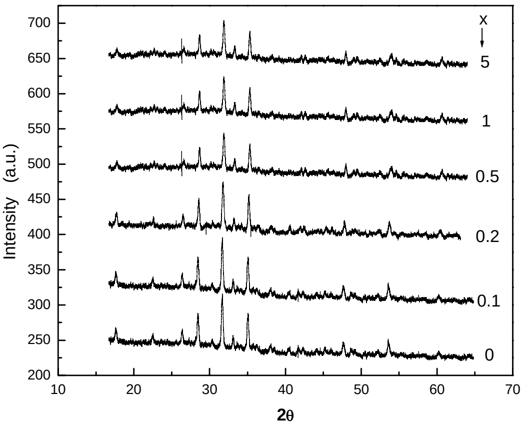

Fig. 3. XRD patterns of the samples after heat treatment at 710℃.

The smallest crystallites were obtained for the hydroxyapatite with a large content of iron and the largest one for calcium iron phosphate.

The ^{31}P MAS NMR experiments were done using a single pulse sequence. The samples have been spun with 8 kHz for obtaining spinning sidebands free spectra. Using a pulse length $\frac{\pi}{2} = 4.4$ microseconds and a intercyclic delay of 100 seconds 1D ^{31}P MAS NMR spectra of HA, HA – 0.1 Fe_2O_3, HA – 0.2 Fe_2O_3 ,HA- 0.5 Fe_2O_3 HA – 1 Fe_2O_3 samples were carried out. Fig. 4 presents the ^{31}P MAS NMR spectra of as prepared samples.

Having in mind the chemical shift range where different structural phosphate units give resonance signals [15], in our as prepared samples only Q_0 phosphorus structural units are formed. The NMR spectrum of undoped sample is a very broad line which appears to be the contribution of three distinct Q_0 units, which present differences in bond angle and / or length of P-O bonds. The same kind of phosphorus structural units appears for the doped samples but in completely different fractions, as can be seen in Fig. 4.

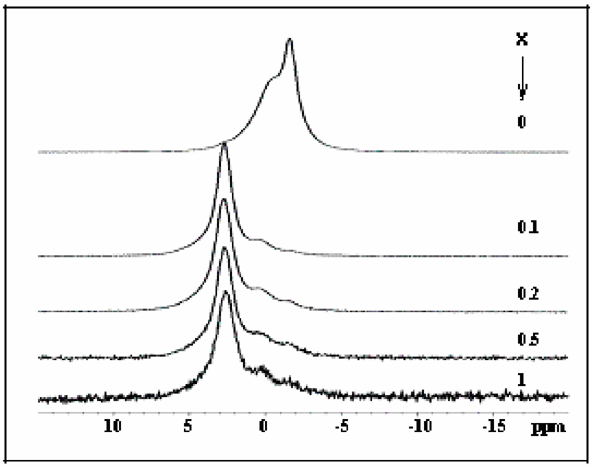

Fig. 4. ^{31}P MAS NMR spectra of the as prepared samples.

In Fig. 5 and 6 are presented the ^{31}P MAS NMR spectra for the samples treated at 300°C and 710°C, respectively.

First heat treatment has as effect a small ordering process, which is release by ^{31}P NMR spectra narrowing process.

The second heat treatment has a completely different effect on analyzed samples. The ^{31}P MAS NMR spectrum of undoped sample presents seven distinctive phosphorus $Q_{(n)}$ units. Unlike in case of untreated and 300 °C heat treated samples, where three Q_0 units with 2.8 ppm, -0.41 ppm and -1.6 ppm appear, in this case only two Q_0 phosphorus units are identified, at 2.78 ppm and -0.4 ppm.

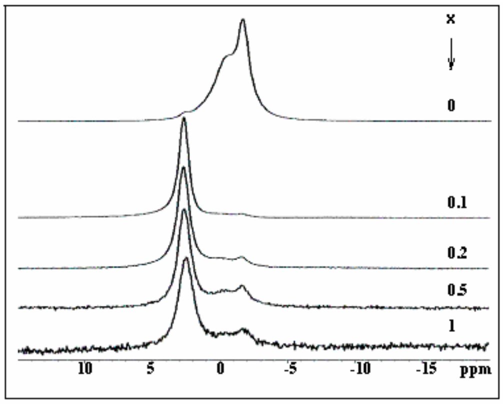

Fig. 5. ^{31}P MAS NMR spectra of samples heat treated at 300°C.

The intensity of this two represents 5.66 % from the total intensity of NMR signal. The other five units are of Q_1 type and represent 94.34 % of signal intensity. These Q_1 phosphorus units give absorptions at -7.05 ppm, -7.99 ppm, -9.03 ppm, -10.25 ppm and -10.87 ppm.

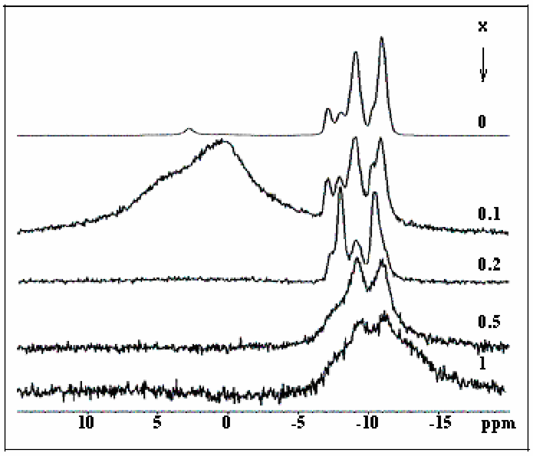

Fig. 6. ^{31}P MAS NMR spectra of the samples after heat treatment at 710°C.

This five phosphorus NMR lines correspond to five interconnected structural units by bridges of oxygen. In these cases one oxygen atom from phosphorus first sphere of coordination is further bonded (O_B) and other three oxygens remain non-bonded (O_{NB}).

Another important difference appears in the case of 0.1 % Fe_2O_3 doped sample where beside the five Q_1 phosphorus units are present very distorted Q_o units that give the broad line in the range from 10 to -5 ppm. The intensity ratio of the Q units is changed dramatically from Q_o/Q_1 = 5.66/94.34 in the iron undoped sample to 71.84/28.16 for the sample with 0.1 % Fe_2O_3.

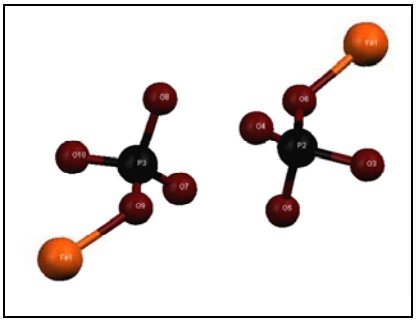

Fig. 7. The vicinity of phosphorus atoms, with one bridged and three non bridged oxygens.

At higher concentrations the effect of iron on the five Q_1 units seems to be more selective. Beside an increase in local disorder, are more affected the Q_1 units with lower chemical shift, that suggest a preferential distribution of iron ions near such units.

4. Conclusions

XRD analysis of iron containing hydroxyapatite powders prepared by sol-gel method revealed the stabilizing effect of iron on hydoxyapatite phase. Even for a very low Fe_2O_3 content the monetit phase developed in iron undoped samples changes to a hydoxyapatite type phase. The ^{31}P NMR spectra show that the phosphorus structural units in nanostructurated units are completely different from those of the microcrystalline samples resulted after higher temperature heat treatment. In the case of nanostructed samples only Q_0 units are present, while in microcrystalline ones the presence of Q_1 units reflects a much interconnected network. At higher iron concentrations the iron ions are preferentially distributed near Q_1 units with lower chemical shift.

Acknowledgements

The authors would like to thank to Gheorghe Vasilie for XRD measurements and useful discussion.

References

[1] D. Arcos, R. P. del Real, M. Vallet-Regi, J. Biomed. Mater. Res. A, **65**, 71 (2003).
[2] D. Eniu, D. Cacaina, M. Coldea, M. Valeanu, S. Simon, J. Magn. Magn. Mat. **293**, 310 (2005).
[3] L. L. Hench, J. Am. Ceram. Soc. 1705 (1998).
[4] N. Y. Mostafa – Mat. Chem.& Physics 94 333 (2005).
[5] H. Wang, N. Eliaz, Z. Xiang, H-Ping Hsu, M. Spector, L. W. Hobbs, Biomaterials **27**, 4192 (2006).
[6] F. N. Oktar, Mat. Lett. **60**, 2207 (2006).
[7] W. Jen, M. Chin, J. Crystal Growth **275**, 2339 (2005).
[8] J. M. Gomez-Vega, E. Saiz, A. P. Tomsia, G. W. Marshal, S. J. Marshall, Biomaterials **21**, 105 (2005).
[9] M. Y. Shareef, P. F. Messer, R. Van Noort, Biomaterials **14**, 69 (1993).
[10] A. I. Villacampa, J. M. Garcia-Ruiz, J. Crystal Growth **211**, 111 (2000).
[11] A. D. Papargyris, A. I. Botis, S. A. Papargyri, Key Eng. Mater. **83**, 206 (2002).
[12] Y. Liva, W. Wanga, Y. Zhana, C. Zhenga, G. Wanga, Mat. Lett. **56**, 496 (2002).
[13] S. Overgaard, Acta Orthop. Scand. **71**, 1 (2000).
[14] B. I. Lazonyak, V. A. Morozov, A. A. Belik, S. S. Khasanov, V. Sh. Shekhtman, J. Solid State Chem. **122**, 15 (1996).
[15] R. K. Brow, J. Non-Cryst. Solids 263&264, 1 (2000).

---

[*] Corresponding author: mc3313@yahoo.com